IOP Conf. Series: Materials Science and Engineering **423** (2018) 012136 doi:10.1088/1757-899X/423/1/012136

3D Multi-field Coupling Analysis of Three-Phase GIS Bus Bar

Yumei Li[1], Yanbing Li[2], Zhongming Bai[1] , Enlong Wang[1] , Chenghui Yang[1] and Shengguo Zhang[1]

[1]Electrical Engineering College of Northwest Minzu University, Lanzhou, China

[2]HowtoCAE, Beijing, China

Corresponding author: YMLBBD@163.com

Abstract. The temperature in gas insulated bus bars are outcomes of coupled multiphysics field, such as thermal field, fluid field and eddy current field in which skin effect of current plays a considerable role. In this paper, the 3D model of GIS bus bar is established, and the skin effect of current is considered by further fine grids in the calculation to reach accurate loss value. Finite element method and fluid analysis are used to predict the distribution of temperature field of three-phase GIS bus bar.

1. Introduction

The temperature rise for electrical equipment, such as GIS bus bar, disconnector and breaker, is very important for their operating characteristics [1]. The effective temperature prediction of GIS is significant for its structure design. In this paper, the temperature of GIS bus bar is predicted by multi-field coupling analysis.

When the current flows, there is skin effect on the section of GIS bus bars. The skin effect of current, arises from the electromagnetic induction of the current itself, and affects ohmic loss and eddy current loss of conductor in the GIS bus bar at the same time. It is well known that the ohmic loss and eddy current loss is the root of temperature rise of enclosure and insulating gas around the space region in the compartment of GIS [2]. So it is necessary to make sure the loss of conductor and the eddy current loss as accurately as possible[3]. Most of the analysis on prediction of temperature distribution of GIS bus bar has less regard for the skin effect of current, which leads to loss calculation not accurate enough. In this paper, the skin effect is considered under background of further fine meshed grids, and the necessity of fine partitioning is also illustrated through single-phase conductors. Early time, some literature assumes infinite bus, makes 2D analysis, affects the calculation accuracy as well [4].

In this paper, 3D FEM is used to estimate the power loss, the heat transfer relationship between the conduct and enclosure is calculated by the theory of fluid dynamics.

2. Skin effect of current

There is a phenomenon that the current density distributes uneven on the cross section of conductors when alternating current flows, called skin effect. A single conductor model is used to present the calculation of skin effect. It is made by copper with 0.4m in radius and 2m in axial length, where the flowing current is 10kA and 50Hz in frequency. In this model the air domain boundary is far enough to ensure the rationality.

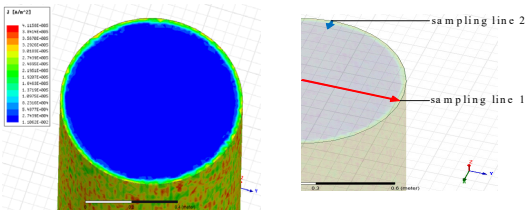

(a) Distribution of current density (b) Sampling line
Figure 1. Single phase conductor model

The deep length of skin effect in this conductor is 9.35mm, which is determined by the frequency, conductivity and magneto conductivity in the following formula:

$$\delta = \sqrt{\frac{2\rho}{\omega\mu}} \qquad (1)$$

In the Figure 1, (a) is about the current density distribution, which shows the current is constrained toward to surface of the conductor and the maximum of current density appears at the edge of the conductor.

However, in the simulated analysis, the mesh generation of the skin effect layer has an inherent influence on the calculation results. While the skin effect area is divided into different grid layer, the results are different. In this paper, Two schemes are compared to explain it. Schemes 1 is the skin effect layer divided into one grid layer and Schemes 2 is the skin effect layer divided into two grid layer. At the same time, two kinds of sampling path shown in Figure1 (b) that are employed to illustrate it. The first sampling line coincides with the positive direction of the Y axis, the length of it equals to the radius of the cylindrical wire while the second goes along the positive direction of the X axis, and the length of it is 20mm, about twice thickness of skin effect layers of the conductor.

The current density of the conductor along path 1 is shown in Figure 2 when the skin effect layer is divided into one grid layer and two grid layer.

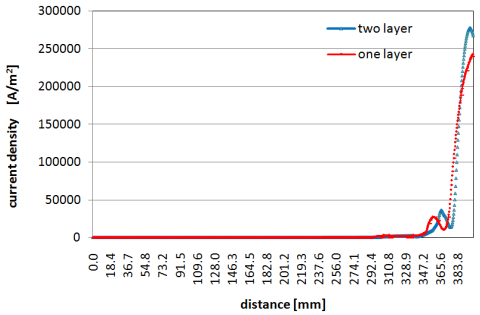

Figure 2. The current density along sample line 1

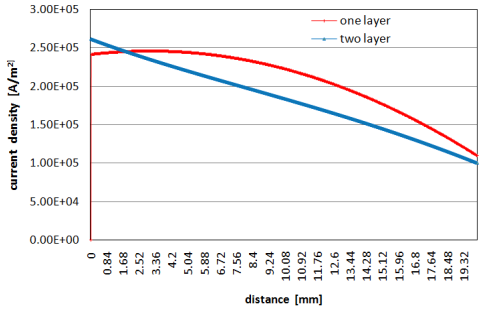

Figure 3. The current density along sample line 2

It can be seen that current density is different near the outer edge, and the maximum of current density also changes correspondingly in the two different grid split scheme. While along path 2 shown in Figure 3, when divided into one layer, the current density of the conductor has a transient increase in the direction from edge points to the center, then decreases immediately, and the whole process is similar to a parabolic shape, when to two layer, the current density goes monotonically decreasing state completely. In the convergence process in this study, the analysis is basically terminated when the electromagnetic energy error is less than 0.007%.

Moreover, the ohmic loss of the conductors is calculated by the two different mesh method. When the depth of skin effect meshed into one grid layer, the heating power values is 66.2 W, when meshed into two grid layer, the ohmic loss is 62.7 W. It can be seen that the result of schemes 2 is smaller, and the relative error is about 5.67% in the two case.

The skin effect is mainly due to the conductor inductance, which is caused by inductance current, and the current is forced to flow crowded along the outer edge of conductor. The further to outward of conductor, the larger about the effect from closed magnetic field that linear related to conductor radius. It goes in accordance with the theory evidence well. As we all know, the finer the division, the more accurate the result of the calculation is. Hence, the skin effect layer that divided into two grid layer is better than one grid layer and multichamber mesh generation is necessary to obtain a satisfactory result. The current density of the single conductor along the radial direction is shown in Figure 4, while eddy current loss density along the radial direction is shown in Figure 5.

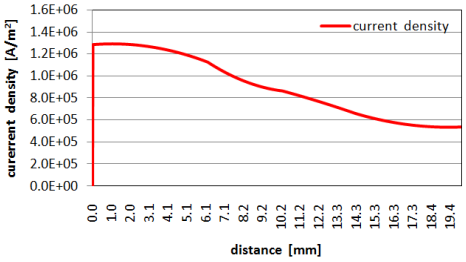

Figure 4. Current density

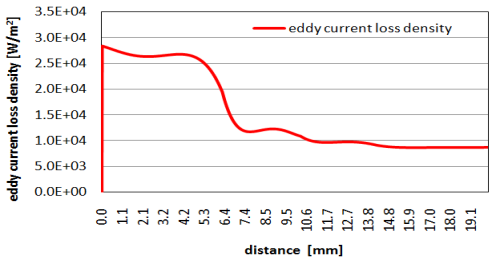

Figure 5. Eddy current loss density

3. Mathematical model

3.1.Electromagnetic Field

The assumptions in this process are as follows:

1.Ignore the displacement current.

2.The current in the conductor is sinusoidal and balanced.

3.The magnetic reluctivity of enclosure and conductors are both constant.

In this GIS bus bar, electric and magnetic fields exist together and influence each other all the time. The relationship between the fields quantities are expressed by Maxwell’ s equations as follows:

$$\nabla \times \vec{H} = \vec{J} \qquad (2)$$

$$\vec{B} = \mu \vec{H} \tag{3}$$

$$\vec{B} = \nabla \times \vec{A} \tag{4}$$

$$\vec{J} = \vec{J}_e + \vec{J}_s \tag{5}$$

$$\vec{J}_e = \sigma \vec{E} = -\sigma(\frac{\partial \vec{A}}{\partial t} + \nabla \phi) \tag{6}$$

Where $\vec{H}$ is magnetic field intensity, $\vec{\mathrm{J}}$ is current density, $\vec{B}$ is flux density, μ is magnetic reluctivity, $\vec{\mathrm{A}}$ is magnetic vector potential, $\vec{\mathrm{J}}_e$ is eddy current density, $\vec{\mathrm{J}}_s$ is source current density, σ is electoral conductivity, ϕ is scalar magnetic potential.

When the effect of harmonic current is ignored, and the Conductivity specification is used, the governing equation becomes:

$$\nabla^2 \vec{A} = \frac{\partial \vec{A}}{\partial t} - \mu \vec{J}_s \tag{7}$$

Applying the Galerkin method to the above equations, the power loss density in each element can be obtained by:

$$P^e = \frac{J^e \, J^{e*}}{\sigma^e} \tag{8}$$

3.2 Fluent-Thermal Field

Fluid flow and heat exchange are common in nature and exist in all kinds of mechanical equipment. In the process of fluid motion and heat transfer, the universal laws must be followed: mass conservation, momentum conservation and energy conservation.

The increase in fluid mass of a unit is equal to the net mass flowing into it in a unit time. Therefore, the continuity equation under the law of conservation of mass is:

$$\frac{\partial \rho}{\partial t} + \nabla(\rho \vec{U}) = 0 \tag{9}$$

Where ρ is fluid density, $\vec{U}$ is fluid velocity, both ρ and $\vec{U}$ are varying with time and spatial position.

Momentum conservation equation:

$$\frac{\partial(\rho u)}{\partial t} + \nabla(\rho u \vec{U}) = \eta \nabla^2 u + S_x - \frac{\partial p}{\partial x} \tag{10a}$$

$$\frac{\partial(\rho v)}{\partial t} + \nabla(\rho v \vec{U}) = \eta \nabla^2 v + S_y - \frac{\partial p}{\partial y} \tag{10b}$$

$$\frac{\partial(\rho w)}{\partial t} + \nabla(\rho w \vec{U}) = \eta \nabla^2 w + S_z - \frac{\partial p}{\partial z} \tag{10c}$$

Where u, v and w are fluid velocity in x, y and z direction, respectively, S_x, S_y and S_z are the sources including distributed resistances and viscous loss terms, p is the gas pressure, and Stokes formulation is used in these equations.

On the basis of Fourier heat transfer law, the energy conservation equation is expressed as :

$$\frac{\partial(\rho T)}{\partial t}+\nabla(\rho\vec{U}T)=\frac{\lambda}{c_p}\nabla^2T+S_T \tag{11}$$

Where T is temperature, λ is coefficient of heat transfer, c_p is the specific heat, S_T is source term include dissipation loss and inner heat source.

As for insulating gas surrounded conductor with current following, heat conduction, convection heat dissipation and thermal radiation are the main form of its heat transfer. In the interior of GIS bus bars, natural convection plays a major role, while effect of the heat radiation can be ignored. On the surface of the enclosure, both thermal radiation and convection are the protagonists. The heat balanced equation is as follows:

$$P_c+P_e=Q_{ec}+Q_{er} \tag{12}$$

$$P_c=Q_{cec}+Q_{cer} \tag{13}$$

Where P_c and P_e are power loss of bus bars and enclosure, respectively, Q_{ec} and Q_{er} are heat spread between enclosure and the surrounding air by convection and radiation. Q_{cec} and Q_{cer} are heat transfer between conductor and enclosure by convection and radiation.

4. Calculations

The three-phase bus bars model calculated in this paper is shown in Figure 6, the air region outer of the enclosure is large enough to ensure the precision. The model is meshed with 768003 elements, while the skin effect region meshed more meticulously by two layers shown in Figure 6 too.

Table 1 the geometry parameters of the model

Classification	Outer diameter (mm)	Inner diameter (mm)	Axial length (mm)
Conductor	70	40	7108
Enclosure	387	376	8912

The geometry parameters of the GIS bus bar are shown in Table 1, both the conductor and the enclosure are made in aluminum. the material parameters of the model at 300 K are shown in Table 2.

Table 2 the material parameters at 300 K

Classification	Thermal conductivity (W/（m·K）)	Specific heat (J/(kg·K))	Viscosity (10^{-5}Pa·s)
Aluminum	2.2	897	-
Air	0.021	1005	18.1
SF_6 gas	0.014	665	1.42

The basic assumptions of the analysis are as follows:

1.Three-phase conductors are triangulated arrangement.

2.The maximum of load current in each phase is 10 kA, and three-phase current are balanced and do sinusoidal changes at frequency of 50 HZ.

3.The GIS is indoor, ignoring the effects of solar radiation.

4.The ambient temperature is 20 ℃ constantly.

5.The initial air pressure is 0.45 MPa.

6.Ignore the effect of basin insulators on convective heat dissipation.

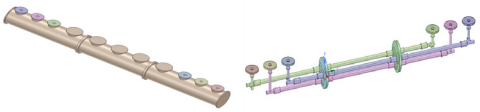

(a) Enclosure (b) Conductors in the enclosure

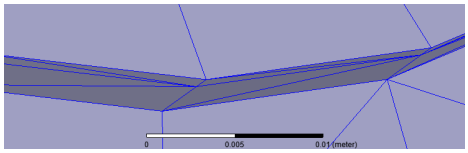

(c) Meshment of skin effect region in the bus bars

Figure 6. Analytical model and the meshment

The distribution of current density in conductors and enclosure is presented in Figure 7. It can be seen that the current density is larger in middle conductors, while the current density of the other two phase conductors are similar. Both the current density of conductors and enclosure are uneven. For the enclosure, the current density is larger on the top of it, because the magnetic fields are affected by stationary components of the GIS bus bar and magnetic lines are squeezed, the current density is smaller at both ends of it, owing to the installation of the conductors is staggered.

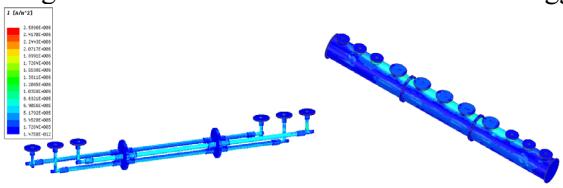

(a) Conductors (b) Enclosure

Figure 7. Current density in conductors and enclosure

The temperature of conductors and enclosure is shown in Figure 8. Although the temperature is different in the three phases but there are similarities that the distribution of the temperature is uneven and the maximum temperature is in the middle. For enclosure, the temperature distribution of it is gradual, the maximum temperature appears on the top of the enclosure, the minimum temperature is at the bottom, and the difference is 22 K. In fact, convection heat is not only driven by temperature difference, but also influenced by gravity. So the convection at the bottom of the enclosure of the GIS bus bar is faster than the top of the enclosure.

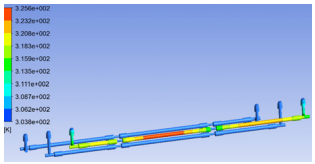

(a) Middle conductor

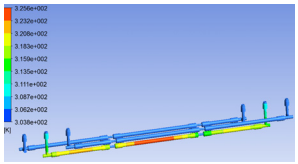

(b) Right side conductor

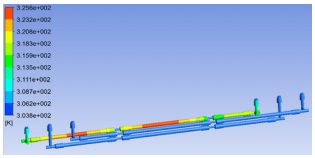

(c) Left side conductor

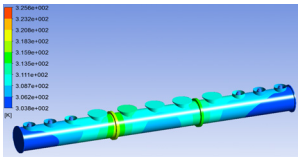

(d) Enclosure

Figure 8. Distribution of temperature

The distribution of the velocity vector for natural convection is shown in Figure 9. Laminar and turbulent flows exist. The flow velocity is larger around the conductor, which is turbulent. When the flow rate is small, it is laminar flow. For the triangulated arranged conductors, the flow velocity is relatively small at the top conductor of the triangle, while the flow velocity around the bottom conductors is larger, because the velocity is affected by the acceleration of gravity. Velocity is higher, heat dissipates rapidly, and the temperature in the region is lower. This corresponds to the temperature distribution.

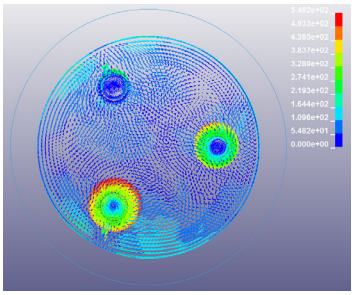

Figure 9. Distribution of the velocity vector

5. Conclusion

In this paper, the 3D model of GIS bus bars is set up, the eddy current field and fluent-thermal were coupled to predict the distribution of temperature and velocity vector. In order to get accurate eddy current loss, skin effect was considered and the skin effect area is further fine meshed. The method of considering the skin effect is described by single phase conductor. Then the loss is used as heat source of fluid analysis. The temperature distribution are highly consistent with the distribution of velocity vector of SF6 gas for the three-phase GIS bus bar.

Acknowledgments

This work was supported by National Natural Science Foundation of china (No.51541710) and the Fundamental Research Funds for the Central Universities (No. 31920170019) .

References

[1] M. Szewczyk, K. Kutorasiński, M. Wroński and M. Florkowski, 'Full-Maxwell Simulations of Very Fast Transients in GIS Case Study to Compare 3-D and 2-D-Axisymmetric Models of 1100kV Test Setup,' IEEE Trans. Power Del., Vol. 32, No.2. (2017).

[2] X.W. Wu, N.Q. Shu, H.T. Li, L. Li, 'Contact Temperature Prediction in Three-Phase Gas-Insulated Bus Bars With the Finite-Element Method,' IEEE Trans. Magn., Vol. 50, No. 2, (2014).
[3] N. Rebzani, E. Clavel, P. Marty, A. Morin, 'Numerical Multiphysics Modeling of Temperature Rises in GAS Insulated Busbars,' IEEE Trans. Diel Elect Insulation, Vol. 23, No. 5. (2016).
[4] H.K. Kim, Y.H. Oh, S.H. Lee, 'Calculation of Temperature Rise in Gas Insulated Busbar by Coupled Magneto-Thermal-Fluid Analysis,'J. Elect Eng.Technol., Vol. 4, No. 4, (2009).
[5] Sumedh Pawar, Kishor Joshi, Lalichan Andrews, and Subodh Kale, 'Application of Computational Fluid Dynamics to Reduce the New Product Development Cycle Time of the SF6 Gas Circuit Breaker', IEEE Trans. Power Del., Vol. 27, No. 1 (2012).
[6] Jasmin Smajic, Walter Holaus, Jadran Kostovic, and Uwe Ridchert, '3D Full-Maxwell Simulations of Very Fast Transients in GIS', IEEE Trans. Magn., Vol. 47, No.5, (2011).
[7] Joong Kyoung Kim, Sung Chin Hahn, Kyong Yop Park, Hong Kyu Kim, and Yeon Ho Oh, 'Temperature Rise Prediction of EHV GIS Bus Bar by Coupled Magnetothermal Finite Element Method', IEEE Trans. Magn., Vol. **41**, No. 5, (2005).
[8] S. L. Ho, Y. Li, X. Lin, Edward W. C. Lo, K. W .E. Cheng, and K. F. Wong, 'Calculations of Eddy Current, Fluid, and Thermal Fields in an Air Insulated Bus Duct System', IEEE Trans. Magn., Vol. **43**, No.4, (2007).